Materials Today Bio 15 (2022) 100332

Contents lists available at ScienceDirect

Materials Today Bio

journal homepage: www.journals.elsevier.com/materials-today-bio

Mechanism assay of interaction between blood vessels-near infrared probe and cell surface marker proteins of endothelial cells

Muhammad Asri Abdul Sisak [a], Fiona Louis [b], Tomoyuki Miyao [c], Sun Hyeok Lee [d,e], Young-Tae Chang [d,f], Michiya Matsusaki [a,*]

[a] Department of Applied Chemistry, Graduate School of Engineering, Osaka University, Osaka, 565-0871, Japan
[b] Joint Research Laboratory (TOPPAN) for Advanced Cell Regulatory Chemistry, Graduate School of Engineering, Osaka University, Osaka, 565-0871, Japan
[c] Data Science Center, Nara Institute of Science and Technology (NAIST), Nara, 630-0192, Japan
[d] Center for Self-assembly and Complexity, Institute for Basic Science (IBS), Pohang, 37673, Republic of Korea
[e] School of Interdisciplinary Bioscience and Bioengineering, Pohang University of Science and Technology (POSTECH), Pohang, 37673, Republic of Korea
[f] Department of Chemistry, Pohang University of Science and Technology (POSTECH), Pohang, 37673, Republic of Korea

ARTICLE INFO

Keywords:
Fluorescent probes
Endothelial cells
CD133 protein
Live imaging

ABSTRACT

In vivo blood vessels imaging is crucial to study blood vessels related diseases in real-time. For this purpose, fluorescent based imaging is one of the utmost techniques for imaging a living system. The discovery of a new near-infrared probe (CyA-B2) by screening chemical probe library in our previous report which showed the most specific binding on the blood capillaries of the 3D-tissue models give us interest to study more about the binding site of this probe to the surface of endothelial cells main component cell of blood capillaries. By studying the competition assays of CyA-B2 using several potential surface markers of endothelial cells found through the chemical database (ChEMBL) and manually selected, CD133 gave the lowest IC_{50} (half maximal inhibitory concentration) value. Hence, CD133 protein which is expressed on the endothelial cell membrane was postulated to be the binding site due to the suppression of CyA-B2 on the blood capillaries by the competition assays. Since, CD133 is also expressed on many types of cancer cells, it would be useful to use CyA-B2 as a bioprobe to monitor or diagnostic tumor growth.

1. Introduction

As widely known the function of blood vessels is to deliver oxygen and nutrients for tissues and organs as well as transporting blood throughout our body. There are many diseases which are related to blood vessels such as atherosclerosis, ischemia and so on [1]. Since organs in our body are not directly visible, *in vivo* blood vessels imaging is required to investigate their structure and perform real-time detection. By using fluorescence, it may help to visualize specific area or cells in real-time. As one of the widely used fluorescent labeling compounds, fluorescent probes have many advantages, such as fast detection speed, good repetitiveness, low dosage, and non-radiation [2–4]. Many studies have been done to perform live-cell imaging whether *in vitro* or *in vivo* applications, targeting specific cells or response to different environment by using organic fluorescent probes [3,5–7].

Conventional method to design fluorescent probe are based on the specific target molecule. However, the fluorescent probe sometimes does not guarantee to work very well when applied in the real application or clinical trial due to several problems such as biological complexity in living systems and off-target effect due to low stability in the blood stream [8,9]. An alternative method is to generate multiple probes, without knowing the target in advance, by using a fluorescent probe library consisting of diverse structures, and then screen their potential targets [10,11]. Screening of fluorescent libraries can produce interesting fluorescent ligands that lead to the discovery of novel mechanisms and reveal new biological processes [12,13]. Using this method, in our previous study, we screened chemical probes containing diversity structures in a library format to find a new fluorescent probe for live-blood capillary imaging at near-infrared (NIR) wavelength range [14].

For this step, it is very important to select the most accurate screening system to achieve reliable result when applied in *in vivo* systems. Several studies for screening chemical probes have been done in 2D cell culture. However, 2D culture is different from 3D systems which in turn leads to misleading results when applied in *in vivo* tissues. To improve the

* Corresponding author. Department of Applied Chemistry, Graduate School of Engineering, Osaka University, Suita, Osaka, 565-0871, Japan.
E-mail address: m-matsus@chem.eng.osaka-u.ac.jp (M. Matsusaki).

https://doi.org/10.1016/j.mtbio.2022.100332
Received 7 May 2022; Received in revised form 13 June 2022; Accepted 16 June 2022
Available online 23 June 2022

applicability of probes to tissue staining, it may be the most straightforward to directly use tissues for the screening. However, it usually means using tissues coming from animal and so the interaction of chemical probe might be different with human native tissues and the screening assay subjected to a low throughput. Therefore, setting up the screening system as similar as possible to the final application is of utmost important consideration in the design of screening systems. Hence, in our group we have developed a new high-throughput screening method using *in vitro* human tissue models for screening the chemical probe library (Scheme 1a and Fig. S1). We fabricated blood capillary models using hydrogel to serve as a 3D system to imitate the complexity of *in vivo* tissues.

In this study, we further investigate the mechanisms of the selected probe (CyA-B2) binding on endothelial cells membrane by cheminformatics approaches, competition binding assay, and photophysical properties of probes by (density functional theory) DFT calculation (Scheme 1b). Endothelial cells express many proteins surface marker [15,16] which might be the potential targets for CyA-B2 binding. Herein, we reported and confirmed the discovery of a novel molecular target for CyA-B2 that is CD133 expressed on endothelial cells [17,18]. Since, CyA-B2 has high binding constant (K_d = 2.4 nM) to CD133, it could be used as a potential theranostic agent for endothelial cells.

2. Materials and methods

2.1. Dynamic light scattering (DLS) measurement

CyA-B2 probe was prepared as previously reported [14]. Briefly, CyA-B2 (1 μM) was mixed with urea and sodium chloride (NaCl) at various concentration in assay buffer (DMEM containing 10% FBS and 1% antibiotics). The mixture was pre-incubated at 37 °C for 20 min prior measurement. Similar concentration of urea and NaCl as in previous report were used (urea: 0, 0.01, 0.1, 0.5 and 1.0 M; NaCl: 0, 1, 10, 50, and 100 mM). DLS (Malvern Zetasizer, Nano ZS Instruments, UK) analysis was measured under 37 °C and the experiments were conducted in triplicate.

2.2. Density functional theory (DFT) calculation

From the screening results of chemical probes that has been done in our previous report [14] and which were then classified as high P′ probes (>1.0E09 a.u.) and low P′ probes (<1.0E09 a.u.). The investigation of the ground and excited state energy of a high P′ and low P' probes and model system were carried out through density functional theory (DFT). The B3LYP/6-31G(d,p) SCRF=(Solvent = Water) and B3LYP/6-31G(d,p) levels of theory were adopted to locate the highest occupied molecular orbital (HOMO) and lowest unoccupied molecular orbital (LUMO) energy level of probes in water and gas phase, respectively. All calculations were performed with the Gaussian 16 software (Gaussian, Inc., Wallingford, CT, USA).

2.3. Target prediction by database screening

Target protein identification was tried by systematic database searching based on the chemical structure of probe molecule CyA-B2. The ChEMBL database (ver. 24); a manually curated bioactive molecule database of more than 1.5 million compounds with biological assay outcome [19] was employed for this purpose. Molecular representation was the extended connectivity fingerprint of bond diameter 4 (ECFP4) [20], folded into a 4096 bit-vector by modulo operation, and the Tanimoto similarity was used as a metric. From standardized molecular structures in the database, molecules similar to CyA-B2 were identified using a similarity threshold of 0.40 based on retrospective similarity searching analyses [21]. For the identified similar compounds, target information was extracted with the following criteria: *target_type* = 'SINGLE PROTEIN', *assay_relationship* = 'D' (direct compound-target interaction) with the highest confidence score of 9, *activity_comment* not 'Not Active' or 'Non-toxic' for avoiding not-active compounds or

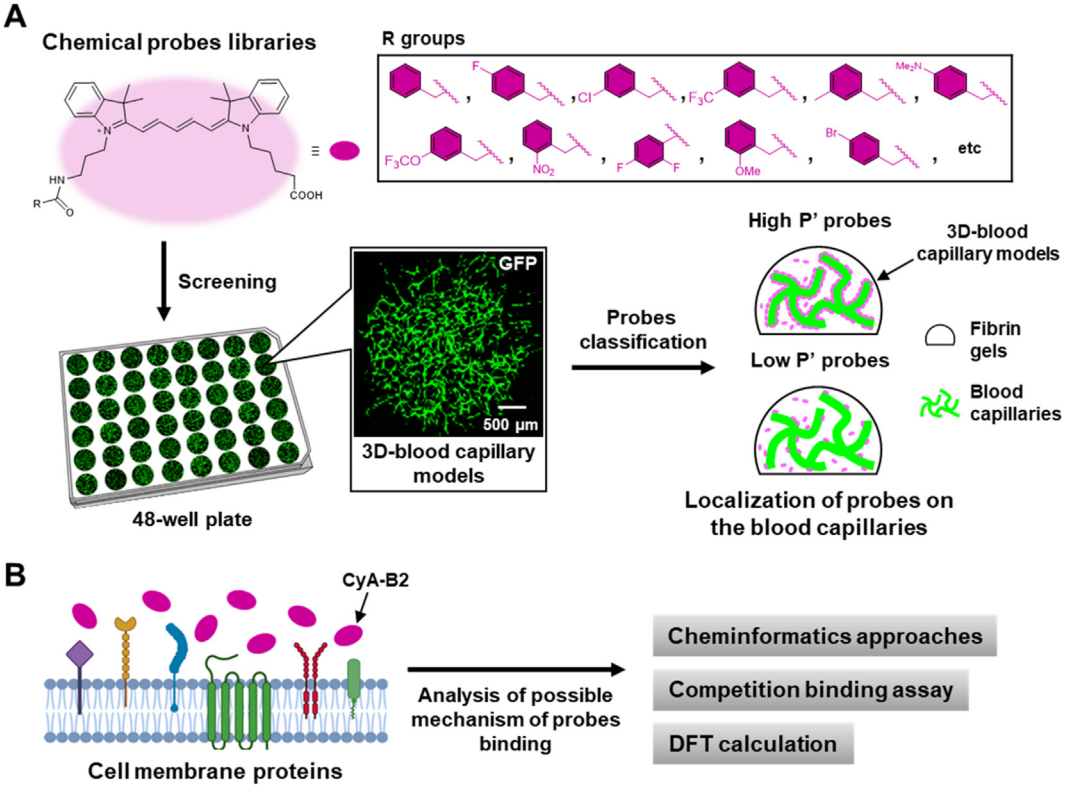

Scheme 1. (a) Illustration of chemical probes screening through *in vitro* blood capillary models to classify higher specific bound probes (high P′) and lower specific bound probes (low P′) on the blood capillaries. (b) Several analyses of possible mechanism of probe binding on the blood capillaries.

targets related to ADMET assays, and *standard_relation* not '>'. From these potential candidate proteins, proteins found in endothelial cells were manually selected as predicted target proteins (Fig. 2a and Fig. S5). The first three target proteins (SNCA, SLCO2B1 and ABCC1) were used for further experiment since they show high expression on endothelial cells based on the Human Protein Atlas [www.proteinatlas.org].

2.4. Competition binding assays

The 3D-blood capillary models were fabricated as described in our previous work [14]. In brief, the 10 μL of fibrin gels which consist of fibrinogen (F8630, Sigma-Aldrich, MO, USA) and thrombin (T4648, Sigma-Aldrich, MO, USA) was mixing with 0.15 mg of collagen microfiber ((Nippon Ham. Foods Ltd., Osaka, Japan), 1.5×10^4 of normal human dermal fibroblast (NHDF, Lonza, Basel, Switzerland) and 7.5×10^3 of green fluorescent protein (GFP) labeled HUVECs (Angio-Proteomie, Massachusetts, USA) and were seeded in 48-well plate, subsequently. Then, the seeded tissues were incubated at 37 °C for 30 min to allow the process of forming a gel. The tissues were cultured for 5 days in a mixed cell culture medium which are Dulbecco's Modified Eagle Medium (DMEM, 08458-45, Nacalai Tesque, Kyoto, Japan) for NHDF and endothelial cell's media KBM VEC-1 basal medium (16030110, Kohjin Bio Co. Ltd, Saitama, Japan. https://kohjin-bio.jp/wp-content/uploads/KBMVEC1_0616.pdf) at ratio 1:1. The mixed culture medium was changed every 2 days. The competition binding assays were done using variety of competitors consisting of specific surface marker for endothelial cells such as anti-CD14 antibody (ab181470, abcam, Cambridge, United Kingdom), anti-CD31 antibody (M0823, Dako, Glostrup, Denmark), anti-CD133 antibody (MA1-219, Thermo Fisher Scientific, Waltham, USA), and mouse IgG (ab37355, abcam, Cambridge, United Kingdom) was used as a control antibody. VEGF-A (226–01781, Wako, Osaka, Japan) and tomato lectin (L-1170-2, Vector Laboratories, Burlingame, CA, USA) which are molecules binding to VEGF receptors and glycoprotein, respectively also expressed on endothelial cells membrane. Alpha-synuclein (SNCA, MA5-12272, Thermo Fisher Scientific, Waltham, USA) which was obtained from ChEMBL database was also used in this competition assay as it shows highest expression on endothelial cells either from the Human Protein Atlas and also in the 3D-tissues (Fig. S6a, b). All the competitors at various concentration (0, 0.01, 0.1, 0.5, 1.0 μM) were incubated on the 3D-blood capillary models in presence of CyA-B2 (1 μM) for 20 min at 37 °C with 5% CO_2. The tissues were then washed once with phosphate-buffered saline (PBS, D5652, Sigma-Aldrich, MO, USA) prior to live imaging observed by confocal laser scanning microscopy (CLSM, Yokogawa Corp. CQ1). The experiments were conducted in triplicate.

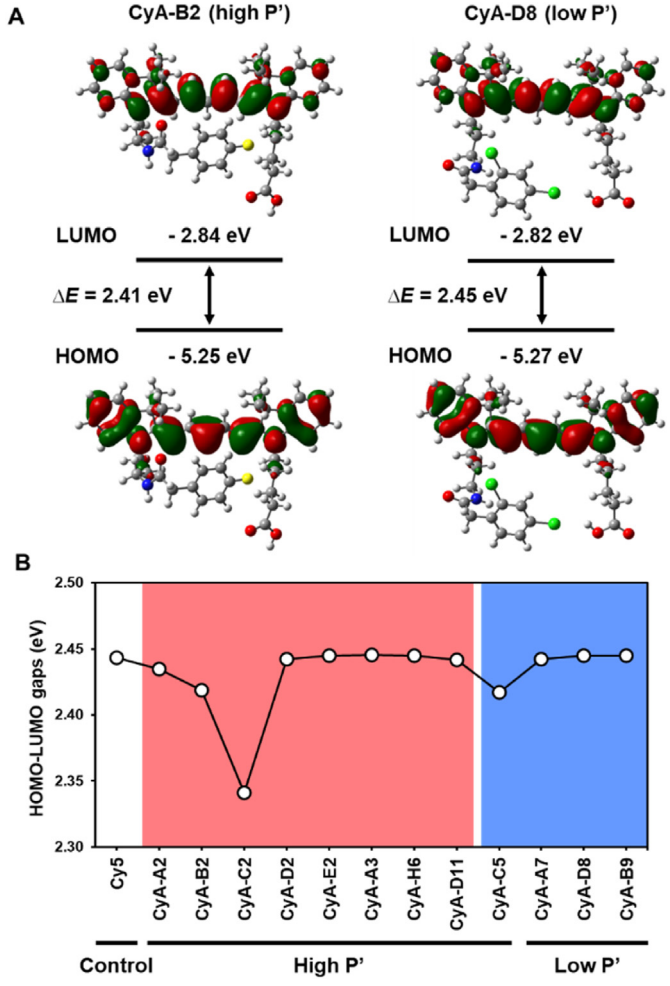

Fig. 1. HOMO-LUMO gaps comparison between high P′ and low P′ probes. (a) Depictions of the HOMO and LUMO of CyA-B2 (high P′) and CyA-D8 (low P′), respectively. (b) Summary of HOMO-LUMO gaps for all high P′ probes (red region) and some of low P′ probes (blue region). Relative energies of the HOMOs and LUMOs are provided in eV.

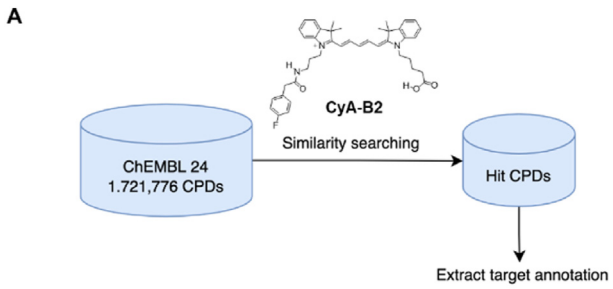

B

Biological targets (related to endothelial cells)	Similarity
Alpha-synuclein (SNCA)	0.44
Solute carrier organic anion transporter family member 2B1 (SLCO2B1)	0.40
Multidrug resistance-associated protein 1 (ABCC1)	0.40
Sphingosine 1-phosphate receptor 2 (S1PR2)	0.44
Histamine H_2 receptor (HRH2)	0.48
Glutamate carboxypeptidase 2 (FOLH1)	0.49

Fig. 2. Analysis of screened chemical probes by informatics or machine learning approaches. (a) The procedure for target prediction of CyA-B2 using ChEMBL database and (b) the results of biological targets (related to ECs) which have >~0.4 similarity of structure with CyA-B2.

2.5. Immunostaining of antibodies

2.5.1. 3D-tissues

After 5 days culture, the tissues were fixed with 4% paraformaldehyde (09154–85, Nacalai Tesque, Kyoto, Japan) for 20 min at room temperature. The tissues were then washed for 3x with PBS before being permeabilized by 0.2% Triton X-100 (T8787, Sigma-Aldrich, MO, USA) in PBS for 15 min in room temperature. Next, the tissues were washed 3x with PBS and then incubated with 1% BSA-PBS for 1 h in room temperature. The tissues were then ready for being stained with antibody where in our study we used alpha synuclein monoclonal (SNCA) antibody, recombinant anti-multidrug resistance-associated protein (MRP1, also known as ABCC1) antibody (ab233383, abcam, Cambridge, United Kingdom) and solute carrier organic anion transporter family member

2B1 (SLCO2B1) polyclonal antibody (PA5-42453, Thermo Fisher Scientific, Waltham, USA) to investigate the expression of SNCA, MRP1, and SLCO2B1, respectively on the blood capillaries. Anti-CD31 antibody were used as the positive control for expression of endothelial cells on the blood capillaries. All antibodies were diluted at 1:100 in 1% BSA-PBS and were then incubated on the 3D-tissues for overnight at 4 °C. To observe the expression of each antibody, secondary antibody with the fluorescence tag were used. Alexa Fluor 647, anti-mouse (for SNCA) and Alexa Fluor 546, anti-rabbit (for ABCC1 and SLCO2B1) and co-staining with Alexa Fluor 546 (anti-mouse, A-11003, Invitrogen, MA, USA) or Alexa Fluor 647 (anti-mouse, A21235, Invitrogen, MA, USA) for CD31 were diluted in 1% BSA-PBS (1:200) and incubated for 1 h at room temperature. Finally, the tissues were washed 3x with PBS prior to observation with confocal microscopy (CQ1).

2.5.2. 2D monolayer cells

HUVECs and GFP-HUVECs (1×10^5) were seeded on the glass bottom dish (35 mm) and culture for 24 h. After 1 day culture, the cells were washed several times with PBS before fixation process using 4%-PFA. The next step is similar with the method on 3D-tissue above. However, the purpose of this experiment to confirm the expression of CD133 on both types of cells. So, we used anti-CD133 antibody (1:100 dilution in 1% BSA in PBS) to stain the cells and incubated for overnight at 4 °C. After that, Alexa Fluor 546 (1:200 dilution in 1% BSA in PBS) and Hoechst 33342 (H3570, Thermo Fisher Scientific, Waltham, USA, 1:1000 dilution in 1% BSA in PBS) were stained and incubated at room temperature for 2 h. Finally, the cells were washed with PBS before observing the fluorescence using confocal microscope (CQ1).

2.6. Quantification of specific probe adsorption (P')

All the images from CQ1 were taken at 4× magnification which was enough to observe the full image of the blood capillaries in whole tissue. The images were then further analyzed for the quantification of total probe adsorption (P), specific probe adsorption (P′) on the blood capillaries, as well as colocalization (%) by Imaris software (9.1.2 version, Oxford Instruments, Bitplane, Belfast, United Kingdom) as previously described [14,22]. Briefly, using the 'surface' tools on Imaris, the surface for blood capillaries (GFP signal or Alexa Fluor 647-CD31) and probes were constructed according to the fluorescence intensity information. Fluorescence intensity of probe inside the surface of blood capillaries were counted and regarded as specific probes that bound to the blood capillaries (P′). Total probe that bound to the whole tissue (P) were also counted and then the colocalization (%) of the probe was simply assessed by dividing P′ by P value. The threshold for each surface were fixed and were used the same for the whole image analysis. The excitation power and exposure time for acquiring the image from confocal microscope (CQ1) also remained the same (Excitation power: 40%, Exposure time: 300 ms) and were applied to GFP channel (Excitation wavelength: 488 nm) and probe channel (Excitation wavelength: 640 nm).

2.7. IC_{50} values calculation

IC_{50} values (half maximal inhibitory concentration) for each competitor were calculated from the graph of competition binding assays using GraphPad Prism (version 8.0, GraphPad Software, San Diego, CA, USA). All calculation were done using the log (inhibitor) vs response curve-variable slope, three parameters and IC_{50} values were calculated according to the following equation (H. J. Motulsky, "Dose-response-Inhibition", GraphPad Curve Fitting Guide. https://www.graphpad.com/guides/prism/latest/curve-fitting/reg_dr_inhibit_variable.htm):

$$Y = \text{Bottom} + \frac{\text{Top} - \text{Bottom}}{1 + 10\hat{}((\text{LogIC50} - X) \times \text{Hill Slope}}$$

2.8. Binding curve of CyA-B2 and CD133 protein

Various concentration of recombinant human CD133 protein (ab160218, abcam, Cambridge, United Kingdom) from 0.05 to 50 nM were incubated with CyA-B2 (1 μM) in 0.1% DMSO PBS for 5 min at 37 °C. The emission of CyA-B2 was measured by spectrofluorometer at excitation of 640 nm. The experiment also was done to plot the binding curve between low P' probe (CyA-D8) and CD133 protein, CyA-B2 or CyA-D8 and VEGFR1 as control samples. The binding constant (K_d) value from the binding curve was obtained from the Hill equation [23,24].

$$Y = \frac{X}{Kd + X}$$

2.9. Job plot assay

The binding ratio of probe-protein complex was determined by the method of continuous variation (job plot) [25–27]. To the 0.2, 0.4, 0.5, 0.67, 1, 1.33, 1.5, 1.6, and 1.8 μM solution of CD133 protein, 1.8, 1.6, 1.5, 1.33, 1, 0.67, 0.5, 0.4, and 0.2 μM CyA-B2 were added, respectively. The overall concentration of probe and protein added remained constant: [Probe + Protein] = 2 μM. Every test solution had a total volume of 10 μL. After incubation for 5 min, the fluorescence intensities of the samples at 665 nm were measured by a NanoDrop™ 3300 Fluorospectrometer (Thermo Scientific™).

2.10. Statistical analysis

Results are presented as means ± s.d. The sample numbers (n) indicate the number of replicates in the experiment and are provided in the figure legends. Statistical analyses were performed using Excel (Microsoft). The unpaired two-tailed Student's *t*-test was used to determine the significances of differences between groups. $*p < 0.05$, $**p < 0.01$, $***p < 0.001$, N.S. = no significant.

3. Results and discussion

3.1. Electrostatic and hydrogen bonding interaction effects on CyA-B2 distribution

In order to investigate the type of bonding interaction, first the effect of sodium chloride and urea addition was assessed acting as inhibitor of probe interaction to its target through electrostatic interaction and hydrogen bonding respectively, which has been done on the 3D-blood capillary models by staining CyA-B2 in the presence of urea and NaCl in our previous study [14]. In the current report, to further understand the probe interaction, we investigated the distribution of the CyA-B2 probe in presence of increasing concentrations of urea and sodium chloride in order to assess the possible probe-probe interaction (aggregation) inhibiting their binding to the target molecule. Although, in *in vivo* staining we could not analyze the aggregation of CyA-B2 probe due to the presence of many blood proteins (albumin, glycoprotein, lipoproteins, etc.) which might be affecting the distribution of probe, however, the binding ability of the probe to the endothelium layer seemed to be possible anyway due to the visibility of the probe after *in vivo* imaging [14]. From Fig. S2a, the distribution of CyA-B2 in the presence of urea (0–1.0 M) does not change its size indicating that the probe did not aggregate even at higher concentration of urea. Whereas additional of sodium chloride in the buffer (buffer used: DMEM containing 110 mM NaCl) could affect the size of CyA-B2 at 10-fold compared to the size with 0 mM NaCl (110 mM NaCl in DMEM). However, the size of aggregated CyA-B2 are still relatively small (<100 nm) which would not enough to inhibit the probe from reaching the target site [28]. This result might be due to the concentration used in this assay that are not enough to suppress the binding of probe and target via electrostatic interaction. The polydispersity index (PDI) (Fig. S2b) for both experiments show no

different from the control sample (without urea and NaCl) suggesting their homogenous distribution at given concentration of urea and NaCl. Thus, this experiment confirmed the results of no significant difference in the specific binding of CyA-B2 (P 'value) on blood capillaries that has been done in previous reports. The distribution of CyA-B2 probes did not change remarkably following addition of urea and sodium chloride (NaCl), suggesting that the stability of CyA-B2 in both conditions with no binding inhibitions via hydrogen bonding and electrostatic interactions, respectively.

3.2. HOMO-LUMO of high and low P' probes

To get better insight on the differences between classified high P′ probes and low P′ probes, we investigate their photophysical properties by DFT calculation using Gaussian software. Fig. 1a displays the HOMO and LUMO contour plots computed for the CyA-B2 (high P′ value) and CyA-D8 (low P′ value) molecule in the liquid state (water as a solvent). The distribution of HOMO energy and LUMO energy are similar on both CyA-B2 and CyA-D8 molecules, respectively although they are from different class of probes. This results also applied on the other high and low P′ probes (including control molecule, Cy5) as shown in Fig. S3. In order to identify the difference in term of energy level between high P′ probes and low P′ probes, we measured the energy gap of each probe. The HOMO-LUMO gaps (energy level in eV) of high and low P′ probes were calculated and plotted in Fig. 1b, and they showed no clear correlation between high and low P′ probes, even for the molecule of probes in the solid state (Fig. S4). Only CyA-C2 (high P′) showed a relatively lower HOMO-LUMO gap compared to the other probes which might be due to its nature of substituent (NMe_2) that influence the energy level of HOMO [29]. Nevertheless, the screening result of chemical probes in the previous report [14] showed that the P′ value of adsorbed CyA-C2 on the blood capillaries were actually found lower compared to CyA-B2 (the highest one). Overall, these results indicate that the fluorescence properties of the probes do not contribute so much to the results of high and low P 'values and remain unaffected even though each probe consists of different substitutes on the cyanine core structure.

3.3. Prediction of target by similarity searching on the ChEMBL database

With the plethora of data from studies that have been already conducted, prediction of target proteins can be done by searching small molecules similar to CyA-B2 in the ChEMBL database (Fig. 2a). From standardized 1,721,776 unique compounds in the database, 32 similar compounds were identified with Tanimoto similarity values to CyA-B2 between 0.40 and 0.55. For any of the 32 compounds, 43 potential target macromolecules were associated with high confidence of assays. From these potential targets, six endothelial cell-related proteins were manually identified, as shown in Fig. 2b. The corresponding six compounds with Tanimoto similarity values to CyA-B2 and CHEMBL IDs are reported in Fig. S5. From these six targets, SNCA was selected for *in-vitro* testing due to its high expression rate on endothelial cells compared to other proteins based on the Human Protein Atlas data [www.proteinatlas.org] and confirmed in our 3D-blood capillary models (Fig. S6).

3.4. Competition binding assays

To investigate the binding target protein for CyA-B2 present on the vascular endothelial cells, several known endothelial cell surface markers such as CD14, CD31, CD133, alpha-synuclein (SNCA, discovered from ChEMBL database), vascular endothelial growth factor receptor and glycoprotein (Fig. S7a) were chosen as a competition site. The competition assay was performed on the 3D-blood capillary models and the live imaging of the probe were observed by confocal microscopy (CQ1) (Fig. S7b). Live imaging of CyA-B2 was observed for each concentration of CD133 antibody (Fig. 3a, Fig. S8). The fluorescence intensity of the specific adsorption of CyA-B2 (P′) on the blood capillaries were

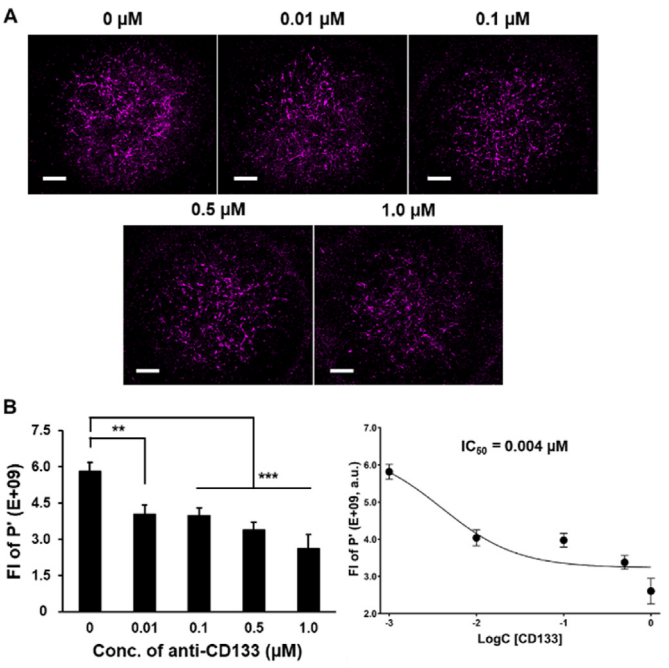

Fig. 3. Competition binding assays of CyA-B2 with proteins or molecules having the same possible target. (a) Confocal images show the effect of CyA-B2 binding without (0 μM) and with (1.0 μM) presence of CD133 during incubation on 3D-blood capillary models. Scale bar is 500 μm. (b) Left graph shows the fluorescence intensity (FI) of specific adsorption (P′) with various concentration of CD133. Data presented as mean ± s.d., (n = 3), $^{**}P < 0.01$, $^{***}P < 0.001$. Right graph shows IC_{50} values from competition assay for CyA-B2 probe with antibodies (IgG, CD14, CD31, CD133, SNCA) and molecules (VEGF-A and tomato lectin).

monitored using Imaris software and plotted with various concentration of CD133 antibody (Fig. 3b, left). It showed that the P′ value of CyA-B2 decreases when increasing the concentration of CD133 antibody, while control IgG (isotype control which does not have specificity to the target but matches the class and type of the primary antibodies used) does not gave a significant difference in the P′ value (Fig. S9a). Then, the IC_{50} value of CD133 antibody competition was calculated by the curve fitting the fluorescence intensity of P' against logarithmic concentration of CD133 (Fig. 3b, right). IC_{50} values for the other competitors were also calculated and were summarized in the Table 1 and Fig. S10. These IC_{50} values of the competition for the CyA-B2 adsorption on the CD133 marker of endothelial cells showed the highest suppression potential on the blood capillaries and was then followed by VEGFR > CD31 > CD14 > SNCA.

The competition binding assays were also done for several other probes used in our previous chemical probes screening results where we classified high P′ probe (CyA-H6) and low P′ probes (CyA-D8 and CyA-C5) (Fig. S11-S16). These competition assays were done using

Table 1
Summary of IC_{50} values for potential competitors using CyA-B2. All IC_{50} values were determined from the graph of P' value.

Competitors	IC_{50} (nM)
Anti-CD133	4.0
VEGF-A	47.0
Anti-CD31	64.0
Anti-CD14	165.6
[a]SNCA	304.6
Tomato lectin	N.D.
IgG	N.D.

[a] SNCA: alpha-synuclein (protein discovered from ChEMBL database); N.D: the data can't be detected from fluorescent titration.

antibodies against CD133 and VEGF-A which had the lowest IC_{50} value from CyA-B2 probe assays. Then, IC_{50} value for each competitor were calculated corresponding to the probes and summarized in the Table 2 and Fig. S17. The results show that CyA-B2 have a lower IC_{50} value compared to CyA-H6 (which also had a high adsorption on the blood capillaries) indicating that CyA-B2 have a higher specificity towards CD133 compared to CyA-H6. In contrast, low P' probes (CyA-D8 and CyA-C5) showed no significant difference from competition binding (Fig. S12 & S13) suggesting no binding site with CD133. Based on this result, we postulated that CyA-B2 binding site was most likely to CD133, and possibly on a similar site that the antibody binding, on the beginning of extracellular part of the protein sequence (https://www.thermofisher.com/antibody/product/Prom1-Antibody-clone-2F8C5-Monoclonal/MA1-219), thus on the endothelial cell membrane and therefore further investigated their binding strength.

3.5. Binding affinity of CyA-B2 and CD133

To confirm the specific interaction between CyA-B2 and CD133, the fluorescence spectra of CyA-B2 (1 μM) in the presence of increasing concentrations of CD133 protein (0–50 nM) was measured (Fig. 4a). From these results, a remarkable fluorescence enhancement of CyA-B2 with increasing concentration of CD133 protein was found, whereas no fluorescence enhancement was observed when CyA-D8 (low P′) was used instead of CyA-B2 with the same concentration of CD133 (Fig. S18). The results suggested that there is a binding event between CD133 protein and CyA-B2 but not for CyA-D8 which proved the specificity of CyA-B2 towards CD133 protein with dissociation constant, K_d = 2.40 nM (Fig. 4b). Furthermore, the job plot assay as shown in Fig. 4c indicated that the binding ratio of CyA-B2 and CD133 protein was measured to be 2:1. To further confirm this specificity with CD133, the same assay was performed in the presence of VEGF-A (0–100 nM) instead (Fig. S19) with CyA-B2 and CyA-D8 (1 μM), respectively. Only a slight fluorescence enhancement was observed for both CyA-B2 (high P′) and CyA-D8 (low P') with increasing concentrations of VEGF-A. These results suggested that there is no specific binding event between VEGF-A with both CyA-B2 and CyA-D8 since the fluorescence intensity shows no significant enhancement. This is in accordance with the IC_{50} values measured in Table 1 showing a limited competitive binding inhibition with VEGF-A.

Table 2
Summary of IC_{50} values for anti-CD133 and VEGF-A as a competitor using high P′ probes (in red) and low P′ probes (in blue), respectively. All IC_{50} values were determined from the graph of P′ value.
N.D: the data can't be detected from fluorescent titration.

Competitors	Chemical probes	IC_{50} (μM)
Anti-CD133	CyA-B2	0.004
	CyA-H6	562.2
	CyA-D8	N.D.
	CyA-C5	N.D.
VEGF-A	CyA-B2	0.05
	CyA-H6	1209
	CyA-D8	N.D.
	CyA-C5	N.D.

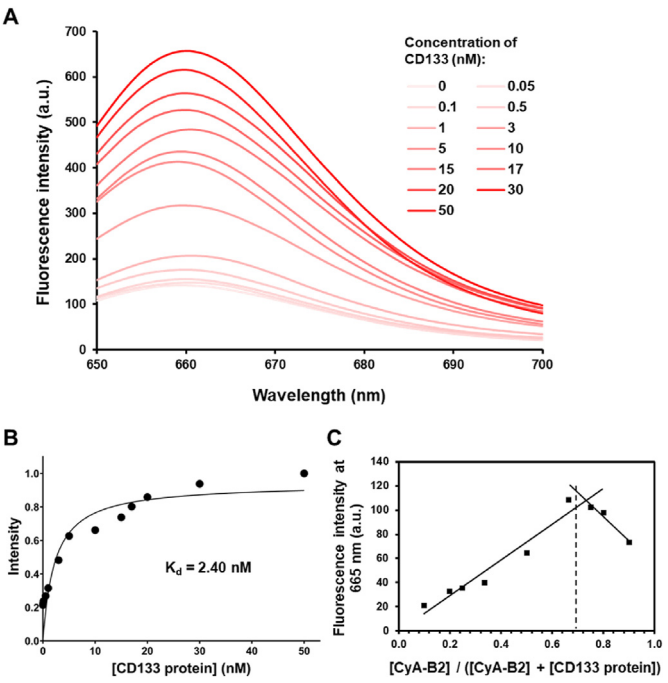

Fig. 4. (a) Fluorescence spectra of CyA-B2 (1 μM) in the presence of CD133 protein. Concentrations of CD133 protein are used from 0.05 to 50 mM. (b) The binding curve illustrates the binding constant (K_d = 2.40 nM) from the curve fitting. (c) Job plot assay for fluorescence intensity at 665 nm of the probe (CyA-B2)-protein (CD133) complex at different molar ratio.

4. Conclusion

In conclusion, we have discussed the mechanisms for the CyA-B2 fluorescent probe which were previously selected from library screening binding on the endothelial cells. The fluorescence properties (HOMO-LUMO) assessment first did not allow to understand any possible correlation. Nevertheless, using the chemical database (ChEMBL) we successfully determined possible target proteins for CyA-B2 and manually selected the one appearing on surface marker of endothelial cells. In this report, we found CD133 expressed on cell surface of endothelial cells (Fig. S20) as a novel target molecule for the probe CyA-B2 binding (Fig. 5). Although, CD133 is not only expressed in HUVEC cells but also in other types of endothelial cells such as endothelial colony-forming cells (ECFCs) and human aortic endothelial cells (HAECs) [18], yet for future applications CyA-B2 could be used as a bioprobe for detecting cells

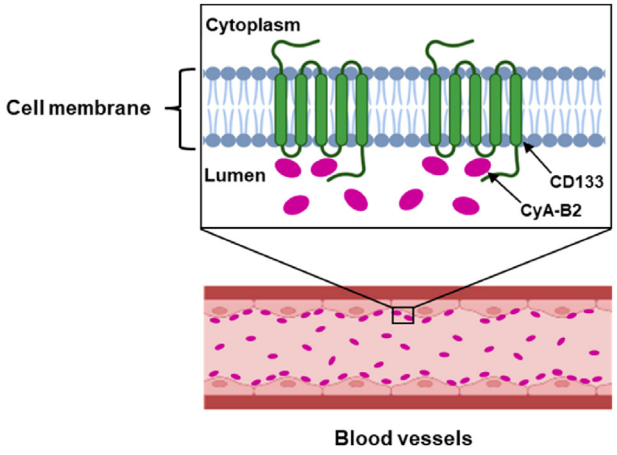

Fig. 5. Schematic illustration of biodistribution of CyA-B2 in blood vessels and their binding site on CD133 protein surface marker of endothelial cells.

expressing CD133 like stem cells [30] and associated with several types of cancer, including some leukemias and brain tumors [31].

Credit author statement

Muhammad Asri Abdul Sisak, Fiona Louis, Tomoyuki Miyao, Sun Hyeok Lee, Young-Tae Chang and Michiya Matsusaki: Conceptualization, Methodology. Sun Hyeok Lee, Young-Tae Chang: Resources. Muhammad Asri Abdul Sisak, Fiona Louis, Tomoyuki Miyao and Michiya Matsusaki: Writing- Original draft preparation. Michiya Matsusaki: Supervision. Fiona Louis, Tomoyuki Miyao: Writing - Review & Editing.

M.A.A.S., F.L., T.M. S.H.L., Y.-T.C. and M.M. conceived and designed the experiments. S.H.L. and Y.-T.C. designed and synthesized the chemical probes. M.A.A.S., F.L. T.M. and M.M. wrote the manuscript, and all authors contributed to the scientific discussion and revised the manuscript. All authors approved the final version of the manuscript.

Declaration of competing interest

The authors declare that they have no known competing financial interests or personal relationships that could have appeared to influence the work reported in this paper.

Acknowledgements

This work was supported by the Grant-in-Aid for Scientific Research (A) (20H00665), Bilateral Joint Research Projects of the JSPS (20199946), JST-MIRAI (18077228) as well as Institute for Basic Science (IBS-R007-A1). Scheme 1b, Fig. 5 and Fig. S7a were made using BioRender.

Appendix A. Supplementary data

Supplementary data to this article can be found online at https://doi.org/10.1016/j.mtbio.2022.100332.

References

[1] P.M. Vanhoutte, H. Shimokawa, M. Feletou, E.H.C. Tang, Endothelial dysfunction and vascular disease – a 30th anniversary update, Acta Physiol. 219 (2017) 22–96, https://doi.org/10.1111/apha.12646.
[2] X. Fei, Y. Gu, Progress in modifications and applications of fluorescent dye probe, Prog. Nat. Sci. 19 (2009) 1–7, https://doi.org/10.1016/j.pnsc.2008.06.004.
[3] X. Liu, Y.T. Chang, Fluorescent probe strategy for live cell distinction, Chem. Soc. Rev. 51 (2022) 1573–1591, https://doi.org/10.1039/d1cs00388g.
[4] J. Zhang, R.E. Campbell, A.Y. Ting, R.Y. Tsien, Creating new fluorescent probes for cell biology, Nat. Rev. Mol. Cell Biol. 3 (2002) 906–918, https://doi.org/10.1038/nrm976.
[5] M. Schäferling, The art of fluorescence imaging with chemical sensors, Angew. Chem. Int. Ed. 51 (2012) 3532–3554, https://doi.org/10.1002/anie.201105459.
[6] Q. Miao, D.C. Yeo, C. Wiraja, J. Zhang, X. Ning, C. Xu, K. Pu, Near-infrared fluorescent molecular probe for sensitive imaging of keloid, Angew. Chem. 57 (2018) 1256–1260, https://doi.org/10.1002/ange.201710727.
[7] H.S. Lv, J. Liu, J. Zhao, B.X. Zhao, J.Y. Miao, Highly selective and sensitive pH-responsive fluorescent probe in living Hela and HUVEC cells, Sensor. Actuator. B Chem. 177 (2013) 956–963, https://doi.org/10.1016/j.snb.2012.12.014.
[8] P. Workman, I. Collins, Probing the probes: fitness factors for small molecule tools, Chem. Biol. 17 (2010) 561–577, https://doi.org/10.1016/j.chembiol.2010.05.013.
[9] J. Blagg, P. Workman, Choose and use your chemical probe wisely to explore cancer biology, Cancer Cell 32 (2017) 9–25, https://doi.org/10.1016/j.ccell.2017.06.005.
[10] N.Y. Kang, H.H. Ha, S.W. Yun, Y.H. Yu, Y.T. Chang, Diversity-driven chemical probe development for biomolecules: beyond hypothesis-driven approach, Chem. Soc. Rev. 40 (2011) 3613–3626, https://doi.org/10.1039/c0cs00172d.
[11] S.W. Yun, N.Y. Kang, S.J. Park, H.H. Ha, Y.K. Kim, J.S. Lee, Y.T. Chang, Diversity oriented fluorescence library approach (DOFLA) for live cell imaging probe development, Accounts Chem. Res. 47 (2014) 1277–1286, https://doi.org/10.1021/ar400285f.
[12] L. Zhang, J.C. Er, K.K. Ghosh, W.J. Chung, J. Yoo, W. Xu, W. Zhao, A.T. Phan, Y.T. Chang, Discovery of a structural-element specific g-quadruplex "light-up" probe, Sci. Rep. 4 (2014) 3776, https://doi.org/10.1038/srep03776.
[13] L. Zhang, J.C. Er, X. Li, J.J. Heng, A. Samanta, Y.T. Chang, C.L.K. Lee, Development of fluorescent probes specific for parallel-stranded G-quadruplexes by a library approach, Chem. Commun. 51 (2015) 7386–7389, https://doi.org/10.1039/c5cc01601k.
[14] M.A. Abdul Sisak, F. Louis, I. Aoki, S.H. Lee, Y.T. Chang, M. Matsusaki, A near-infrared organic fluorescent probe for broad applications for blood vessels imaging by high-throughput screening via 3D-blood vessel models, Small Methods 5 (2021), https://doi.org/10.1002/smtd.202100338.
[15] D. Ribatti, R. Tamma, S. Ruggieri, T. Annese, E. Crivellato, Surface markers: an identity card of endothelial cells, Microcirculation 27 (2020), e12587, https://doi.org/10.1111/micc.12587.
[16] M.C. Munisso, T. Yamaoka, Circulating endothelial progenitor cells in small-diameter artificial blood vessel, J. Artif. Organs 23 (2020) 6–13, https://doi.org/10.1007/s10047-019-01114-6.
[17] U.M. Gehling, S. Leyman Ergü, U. Schumacher, C. Wagener, K. Pantel, M. Otte, G. Schuch, P. Schafhausen, T. Mende, N. Kilic, K. Kluge, B. Schä, D.K. Hossfeld, W. Fiedler, In vitro differentiation of endothelial cells from AC133-positive progenitor cells, Blood 95 (2000) 3106–3112.
[18] E. Rossi, S. Poirault-Chassac, I. Bieche, R. Chocron, A. Schnitzler, A. Lokajczyk, P. Bourdoncle, B. Dizier, N.C. Bacha, N. Gendron, A. Blandinieres, C.L. Guerin, P. Gaussem, D.M. Smadja, Human endothelial colony forming cells express intracellular CD133 that modulates their vasculogenic properties, Stem Cell Rev. Rep. 15 (2019) 590–600, https://doi.org/10.1007/s12015-019-09881-8.
[19] A. Gaulton, A. Hersey, M.L. Nowotka, A. Patricia Bento, J. Chambers, D. Mendez, P. Mutowo, F. Atkinson, L.J. Bellis, E. Cibrian-Uhalte, M. Davies, N. Dedman, A. Karlsson, M.P. Magarinos, J.P. Overington, G. Papadatos, I. Smit, A.R. Leach, The ChEMBL database in 2017, Nucleic Acids Res. 45 (2017) D945–D954, https://doi.org/10.1093/nar/gkw1074.
[20] D. Rogers, M. Hahn, Extended-connectivity fingerprints, J. Chem. Inf. Model. 50 (2010) 742–754, https://doi.org/10.1021/ci100050t.
[21] M. Vogt, D. Stumpfe, H. Geppert, J. Bajorath, Scaffold hopping using two-dimensional fingerprints: true potential, black magic, or a hopeless endeavor? Guidelines for virtual screening, J. Med. Chem. 53 (2010) 5707–5715, https://doi.org/10.1021/jm100492z.
[22] M.A. Abdul Sisak, F. Louis, S. Hyeok Lee, Y. Chang, M. Matsusaki, Fabrication of blood capillary models for live imaging microarray analysis, Micromachines 11 (2020) 727, https://doi.org/10.3390/mi11080727.
[23] A.v. Hill, The possible effects of the aggregation of the molecules of haemoglobin on its dissociation curves, J. Physiol. 40 (1910) iv–vii.
[24] M. Möller, A. Denicola, Study of protein-ligand binding by fluorescence, Biochem. Mol. Biol. Educ. 30 (2002) 309–312. http://www.bambed.org.
[25] P. Job, Formation and stability of inorganic complexes in solution, Ann. Chim. 9 (1928) 113–203.
[26] CharlesY. Huang, Determination of binding stoichiometry by the continuous variation method: the job plot, Methods Enzymol. 87 (1982) 509–525.
[27] S. Lee, D.B. Sung, S. Kang, S. Parameswaran, J.H. Choi, J.S. Lee, M.S. Han, Development of human serum albumin selective fluorescent probe using thieno [3,2-b]pyridine-5(4h)one fluorophore derivatives, Sensors 19 (2019) 5298, https://doi.org/10.3390/s19235298.
[28] E. Blanco, H. Shen, M. Ferrari, Principles of nanoparticle design for overcoming biological barriers to drug delivery, Nat. Biotechnol. 33 (2015) 941–951, https://doi.org/10.1038/nbt.3330.
[29] M. Chemek, S. ben Amor, W. Taouali, E. Faulques, M. Bourass, D. Khlaifia, A. Haj Said, K. Alimi, Photo-physical effects of the chemical insertion of the dimethyl-amine moiety on the newly synthesized oligophenylene (OMPA), J. Mol. Struct. 1241 (2021), 130599, https://doi.org/10.1016/j.molstruc.2021.130599.
[30] Z. Li, CD133: a stem cell biomarker and beyond, Exp. Hematol. Oncol. 2 (2013) 1–8, https://doi.org/10.1186/2162-3619-2-17.
[31] X. Cai, J. Li, X. Yuan, J. Xiao, S. Dooley, X. Wan, H. Weng, L. Lu, CD133 expression in cancer cells predicts poor prognosis of non-mucin producing intrahepatic cholangiocarcinoma, J. Transl. Med. 16 (2018) 1–7, https://doi.org/10.1186/s12967-018-1423-9.